

EFFECTS OF EARTHQUAKE-INDUCED SETTLEMENT OF CLAY LAYER ON THE GROUND SUBSIDENCE

Hiroshi MATSUDA¹, Keiji SAKURADANI² And Naoya EMOTO³

SUMMARY

At the Hyogo-ken Nanbu Earthquake on January 17, 1995, on the artificially reclaimed island, a very large bulk of mud was ejected and the ground subsidence of 30-50cm or more was observed. In this paper, to clarify the effect of earthquake-induced settlement of clay layer on the ground subsidence, firstly the settlement-time relations for the separate layers in the ground which measurement was started from one year before the earthquake are shown and the effects of the earthquake on the settlement of clay layer are investigated. Secondly, the earthquake-induced settlement of the alluvial clay layer in the Port Island was predicted. Thirdly, multi-directional simple shear tests were carried out and the direction of cyclic shear on the settlement of clay layer was observed. In conclusion, following results were obtained. 1) The earthquake-induced settlement of alluvial clay layer of 16m thick reaches over 4cm. 2) When a clay is subjected to the multi-directional shear strain, the larger the phase difference in the sinusoidal shear strains applied from two directions, the smaller the effective stress and therefore the settlement in the reconsolidation stage is affected by the phase difference.

INTRODUCTION

At the Hyogo-ken Nanbu Earthquake, since the large buildings constructed on the artificially reclaimed island was supported by deep foundations, no serious damage to the buildings themselves appeared due to the ground subsidence. However, the differential settlement between the buildings and the surrounding ground affected the lifelines. Usually, it is considered that the earthquake-induced ground settlement is mainly caused by the liquefaction of sandy soil layer [Matsuda, 1996, Lee, 1974, Pyke, 1975, Seed, 1972]. As for the settlement of clay layer induced by the earthquake, it has been shown that the settlement reaches up to 5% in strain and even for the overconsolidated clay the post-earthquake settlement is considerably large compared with the secondary compression. [Ohara and Matsuda, 1988] The fact of the earthquake-induced settlement of clay layer has been confirmed in the 1978 Miyagiken-oki Earthquake [Suzuki, 1984], in the 1957 Mexico Earthquake [Zeevaert, 1972], in the 1985 Mexico Earthquake [Jaime et al., 1987] and in the 1995 Hyogo-ken Nanbu earthquake [Matsuda, 1997]. Especially, after the Hyogo-ken Nanbu Earthquake, the ground surface settled gradually with time. This means that the settlement of clay layer increased by the earthquake, because the settlement induced by the liquefaction of sandy soil takes place immediately after the earthquake. Therefore, the objective of this paper is to clarify the effect of earthquake-induced settlement of clay layer on the ground subsidence in more detail.

¹ Department of Civil Engineering, Yamaguchi University, Tokiwadai, Ube, Yamaguchi, Japan Email: hmatsuda@po.cc

² Department of Civil Engineering, Yamaguchi University, Tokiwadai, Ube, Yamaguchi, Japan Email: yamaguchi-u.ac.jp

³ Maeda Co. Ltd., 4 Watanabe-Dori, Fukuoka, Japan Fax: +81-92-735-0064

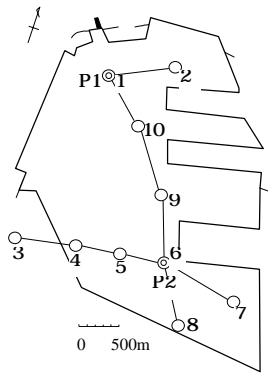


Figure 1: Port Island.

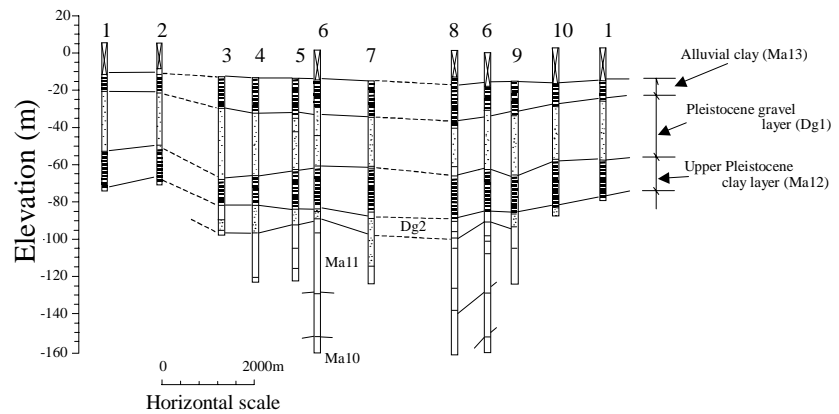


Figure 2: Soil profiles in Port Island.

POST-EARTHQUAKE SETTLEMENT-TIME RELATIONS FOR ALLUVIAL CLAY LAYER

Port Island is a reclaimed island, which is very near to the city center of Kobe, Japan. The soil profiles at the different locations in Port Island are shown in Figure 2, in which the bore hole numbers are the same as those in Figure 1. The depth of the original seabed at the location of Port Island was 10-13m. The alluvial clay layer of 10-20m thick (Ma13) lies beneath a reclaimed stratum and underlain by laminated gravel sand layers (Dg1) which include thin silt and clay layers. The upper part of this laminated layer permits drainage from the alluvial clay and also supports bearing piles. The upper Pleistocene clay layer of 20-30m thick (Ma12) lies beneath the laminated layer. In Figure 2 soil profiles for Nos. 1, 10, 9, 6 and 8 show that toward the south, the surface of the alluvial clay layer (Ma13) slopes and its thickness increases. Soil profiles Nos. 3, 4, 5, 6 and 7 show that the thickness of the alluvial clay layer toward the east is almost the same, but there is a tendency that the thickness of the upper Pleistocene clay layer (Ma12) increases. [Matsuda et al., 1996]

In Figure 3, the changes in the liquid limit w_L , plastic limit w_p , natural water content w_n , void ratio e , unconfined strength q_u , consolidation yield stress P_c and compression index C_c are shown. The samples were obtained around the center of the north part of the Port Island between 1975 and 1977 [Tanimoto, 1989], when the first stage of the reclamation work had been finished. Now, the second stage of reclamation work is under construction in the south part of Port Island.

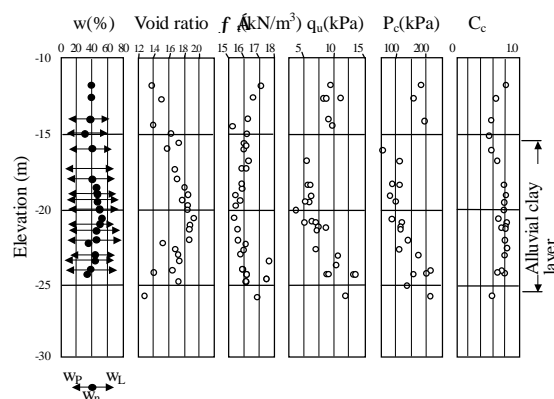


Figure 3: Characteristics of alluvial clay on Port Island. [Tanimoto, 1989]

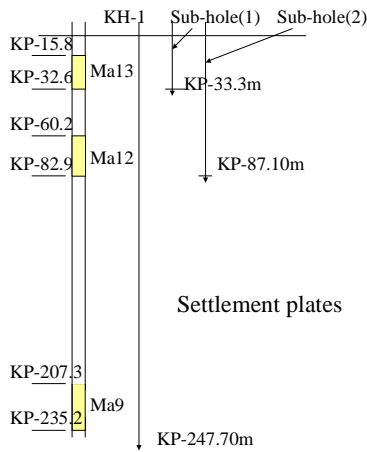


Figure 4: Positions of settlement plate.

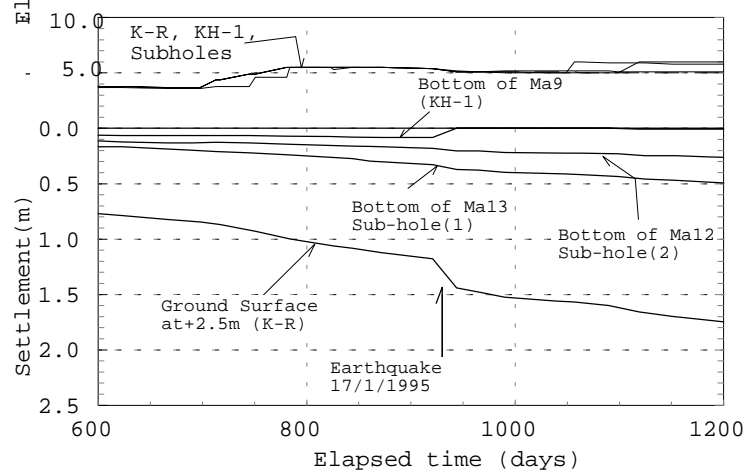


Figure 5: Settlement-time relations for the different depths in Port Island.

At the point P2 in Figure 1, which is located in the second reclamation work site in Port Island, the settlements were measured at four different depths as shown in Figure 4; Plate(1) was placed at the ground surface (k.P.+2.5m), Plate(2) was placed at just under the alluvial clay layer Ma13 (K.P.-33.3m), Plate(3) was placed at just under the upper Pleistocene clay layer Ma12 (K.P.-87.1m), Plate(4) was placed at just under the lower Pleistocene clay layer Ma9 (K.P.-247.7m). The measurement of settlement was started on July 3rd 1992. In Figure 5, the settlement-time relations for each settlement plate are shown. At the ground surface, the significant settlement occurs by the earthquake. This is mainly due to the recompression of liquefied soil as mentioned above. Figure 6 shows the settlement-time curves, in which the fixed line is the result by the Plate(1) at the ground surface. It is seen that by the earthquake, the settlement of about 26 cm occurred. Curve I in Figure 6 is the predicted result by considering that the earthquake didn't occur and Curve II was obtained by moving Curve I down to pass through the first data point obtained after the earthquake. When comparing the Curve II and the observed curve, after the earthquake, the observed settlement is larger than the Curve II. This means that the earthquake affects the settlement-time relations of clayey layer, because the settlement induced by the liquefaction of sandy soil must occur in a very short period.

The earthquake-induced settlement of clay layer with different plasticity indices has been predicted based on the simple shear test results [Matsuda and Nagira, 1998]. Figure 7 shows the relationships between the shear strain amplitude and volumetric strain for the number of strain cycles of 200. The samples used in the test are Kaoline, Yanai clay, Ariake clay, Onoda clay. The physical properties of these samples are shown in Table 1.

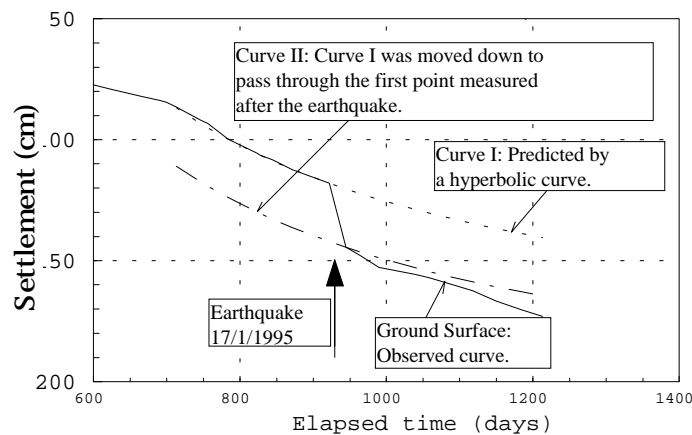


Figure 6: Settlement-time relations at the Port Island. Kobe. [Matsuda, 1997]

Table 1: Physical properties of clay samples used in a series of tests.

	Kaoline	Yanai clay	Ariake clay	Onoda clay
G_s	2.718	2.661	2.629	2.628
w_L (%)	47.4	77.4	67.6	81.1
w_p (%)	31.0	28.9	17.0	27.2
I_p	16.4	48.4	50.6	52.9

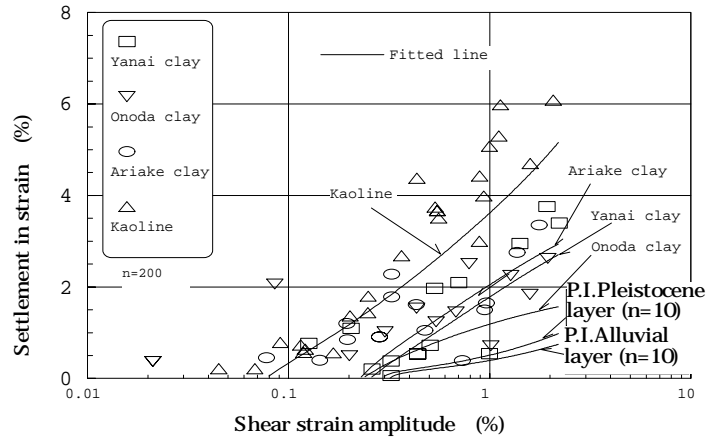


Figure 7: Volumetric shear strain induced by cyclic shear strain.

Table 2: Settlement of alluvial clay layer in Port Island induced by the 1995 Hyogo-ken Nanbu earthquake.

Component of Earthquake	Thickness (m)	Settlement in strain (%)	Settlement (cm)
EW		0.21	1.67
NS		0.52	4.16

Since the details of the method to predict the earthquake-induced settlement have been shown [Matsuda et al., 1998], for the alluvial clay layer in Port Island it is possible to calculate the settlement induced by the 1995 Hyogo-ken Nanbu Earthquake. In Table 2, the earthquake-induced settlement of alluvial clay layer for the EW and the NS components of the earthquake motion are shown. The settlement of the alluvial clay layer is 4.2 cm for the NS component and 1.7 cm for the EW component. Since the settlement of the ground surface which occurred in a very short period was 26.8 cm as shown in Figure 1, the additional settlement of about 4 cm must occur after the earthquake. The difference in the predicted settlement for the EW component and NS component of the earthquake motion is very large. Therefore, the effects of direction of the earthquake motion on the post-earthquake settlement are discussed in the following paragraph.

EFFECTS OF DIRECTION OF EARTHQUAKE MOTION ON THE SETTLEMENT OF CLAY LAYER

The Hyogo-ken Nanbu earthquake of January 17, 1995 has been assigned a JMA magnitude of 7.2 by the Japan Meteorological Agency. At the site designated as P1 in Figure 1, the seismographs were set up at four different depths as shown in figure 8 [GEORK, 1995]. The seismoscope traces recorded at the depth of 16m are shown in Figure 9. It is seen that the direction of the maximum acceleration is toward SE.

As mentioned above, the method to predict the post-earthquake settlement of clay layer has already been shown [Matsuda and Ohara, 1990, Matsuda, 1997]. But the effect of direction of earthquake motion was not taken into account in the prediction method. As for the earthquake-induced settlement of sandy layer, the effects of the multi-directional loading have been investigated. [Pyke et al., 1975, Nagase and Ishihara, 1988] So, in this study a multi-directional simple shear test apparatus as shown in Figure 10 was newly developed and a clay specimen was subjected to the sinusoidal shear strain from two directions, which are perpendicularly intersecting at the center of the specimen. In a series of tests, the shear strain amplitude and the phase angle of cyclic shear strain

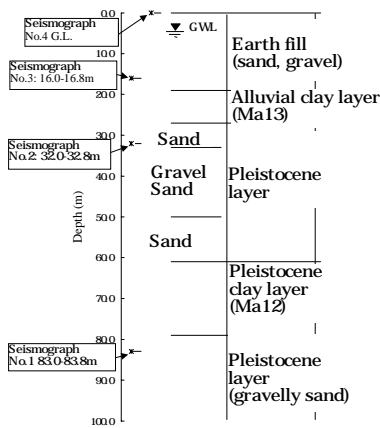


Figure 8: In situ condition where the seismographs were set

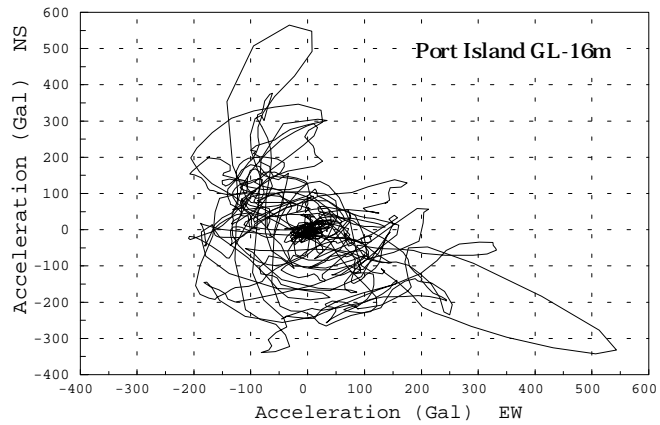


Figure 9: Seismoscope traces recorded during 1995 Hyogo-ken Nanbu Earthquake.

for each direction were changed and the effects of the phase difference of cyclic shear strain on the excess pore water pressure and on the settlement were investigated.

Sample and Test Method

After the end of consolidation of a saturated specimen (60 mm in diameter, 200mm in height) by the consolidation stress of $\sigma_{vo} = 49$ kPa, the cyclic shear strain which faces toward X-direction and Y-direction as shown in Figure 11 was applied under the constant volume condition. The wave form of cyclic shear strain is sinusoidal. In a series of tests, the phase difference θ in the cyclic shear strain of X-direction and that of Y-

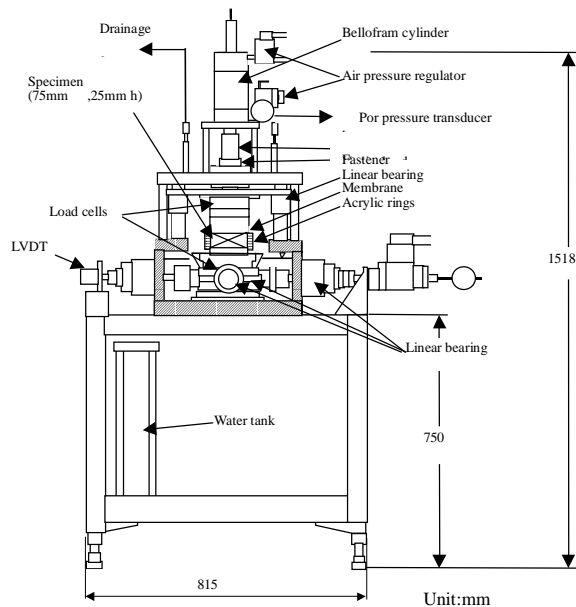


Figure 10: Multi-directional simple shear test apparatus.

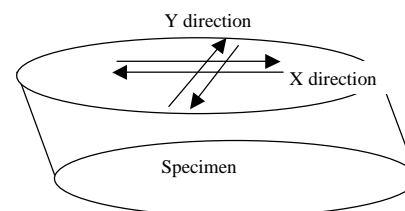


Figure 11: Direction of cyclic shear strain.

direction was changed as $\theta = 0^\circ, 20^\circ, 45^\circ$ and 90° . The sample used in this study was Kaoline as shown in Table

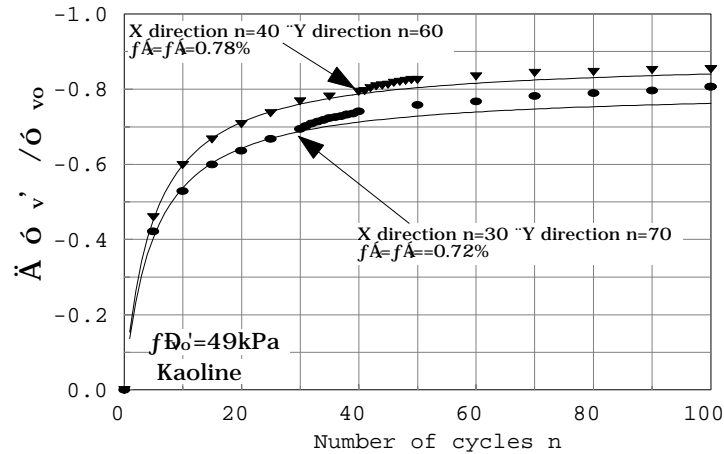


Figure 12: Effect of direction of cyclic shear strain on the reduction in effective stress.

1. After the cyclic shear test, the specimen was reconsolidated under the vertical stress of $\sigma_{vo}=49$ kPa. The period of cyclic shear was fixed as 2.0s and the shear strain amplitude in the X-direction γ_X and Y-direction γ_Y were changed in the range from 0.05 to 2.0%.

Decrease in Effective Stress Induced by Cyclic Shear

Before starting the series of tests, a special test was carried out, in which after the specimen was subjected to the cyclic shear toward X-direction for 30 cycles, the additional cyclic shear toward Y-direction was applied for 70 cycles with the same shear strain amplitude as X-direction. During cyclic shear test, the volume of specimen was kept constant and the change in the vertical stress $\Delta\sigma_v$ was measured. In Figure 12, relationships between $\Delta\sigma_v / \sigma_{vo}$ and the number of cycles are shown. In the same figure, the results for the other number of cycles as 40+60 are also shown. When the direction of cyclic shear was changed, it is seen that the value of $|\Delta\sigma_v / \sigma_{vo}|$ decreases. This means that the direction of cyclic shear have some effects on the excess pore water pressure accumulated during the earthquake.

Typical records of shear strain-time relations for the multi-directional cyclic shear test for $\theta=90^\circ$ are shown in Figure 13. In Figure 14, traces of the cyclic shear strain for $\theta=0^\circ, 20^\circ, 45^\circ$ and 90° at the 50th cycle are shown. In the case of $\theta=0^\circ$, the trace forms the linear line and therefore this case corresponds to the simple shear test. In the case of $\theta=90^\circ$ the trace forms the circle line and this case corresponds to the gyratory shear test which was called by Pyke et al., [1975].

In this study the shear strain amplitude and the phase difference during the cyclic shear test were changed as mentioned above. The relations between $\Delta\sigma_v / \sigma_{vo}$ and the major shear strain amplitude γ_M , for the number of cycles $n=50$ are shown in Figure 15, where γ_M is defined as the half of the major axis on the ellipse which is traced by the shear strains in the X and Y directions. For example, when the cyclic shear strain amplitude toward X-direction and that toward Y-direction are the same as $\gamma_X = \gamma_Y$, γ_M is obtained as $\gamma_M = \sqrt{2} \cdot \gamma_X = \sqrt{2} \cdot \gamma_Y$.

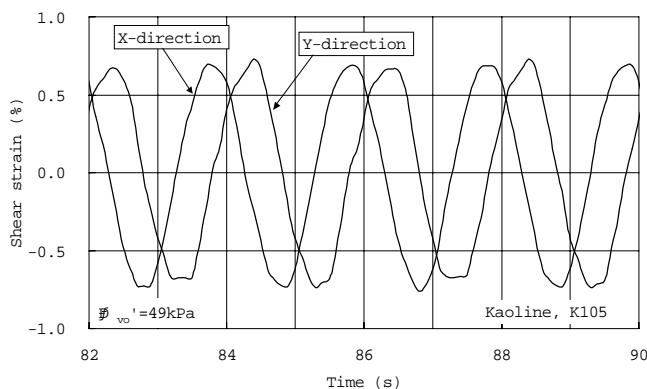


Figure 13: Typical records of shear strain-time relations in the multi-directional simple shear test.

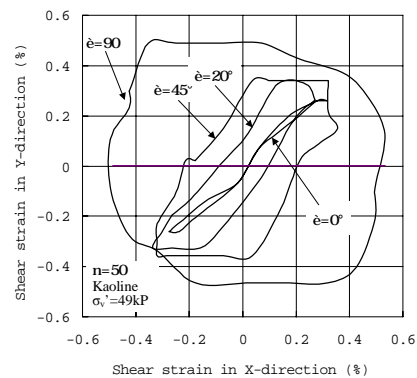


Figure 14: Traces of the cyclic shear strain for $\theta=0^\circ, 20^\circ, 45^\circ$ and 90° .

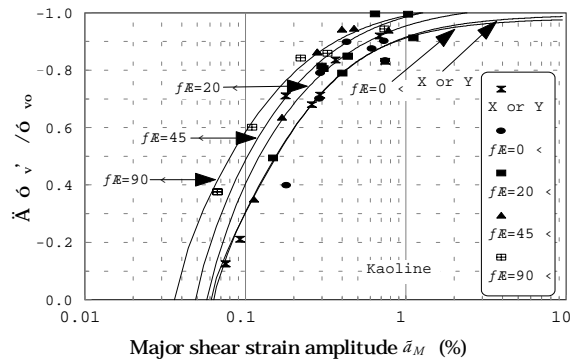


Figure 15: Relationships between shear strain amplitude and the change in vertical effective stress.

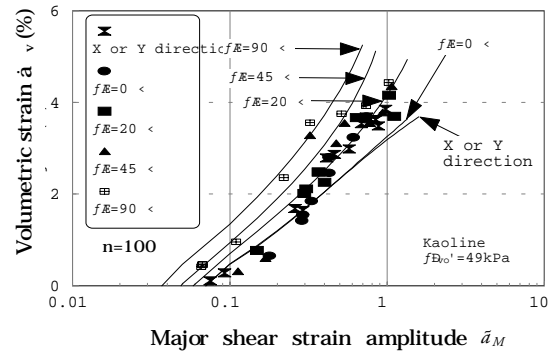


Figure 16: Settlement induced by multi-directional cyclic shear strain.

Plots in Figure 15 are the observed results and the fixed lines are obtained by the following equation [Ohara and Matsuda, 1988, Matsuda and Nagira, 1998].

$$\Delta \sigma'_v / \sigma_{vo} = \frac{-n}{A \cdot \gamma_M^m + n \cdot \gamma_M / (B + C \cdot \gamma_M)} \quad (1)$$

where A, B, C and m are the experimental constants. In Figure 15, a close agreement between the observed plots and the calculated lines was obtained. Although Equation (1) was derived for the simple shear test condition, it is possible to apply to the multi-directional simple shear test results. Furthermore, it is seen that the larger the phase difference, the larger the value $|\Delta \sigma'_v / \sigma_{vo}|$.

Settlement induced by the multi-directional cyclic simple shear

When the excess pore water pressure accumulated during the cyclic shear dissipates, the settlement occurs. In Figure 16, relationships between the major shear strain amplitude γ_M and the volumetric strain ϵ_v for different phases are shown. Data plots in the figure are observed results and curves were obtained by the following equation.

$$\epsilon_v = \frac{C_{dyn}}{1 + e_o} \log \frac{1}{1 + \Delta \sigma'_v / \sigma_{vo}} \quad (2)$$

where e_o is the initial void ratio and C_{dyn} is the dynamic compression index. In Figure 16, when the phase difference increases, larger settlement occurs. For the post-earthquake settlement of sand layer, two opposite results have been reported, the one is that the maximum shear strain induced during the irregular loading is uniquely correlated with the volumetric strain during the reconsolidation [Nagase et al., 1988] and the other is that the multi-directional shaking can apparently increase settlements to as much as three times the settlements caused by shaking in one direction only [Pyke et al., 1975].

The results obtained in this study show that when a clay is subjected to the multi-directional shear strain, the settlement in the reconsolidation stage is affected by the phase difference. Therefore the settlement of the alluvial clay layer in Port Island as shown in Table 2 which was calculated for the one component of the earthquake motion should be corrected. Then the larger result for the post-earthquake settlement would be obtained.

CONCLUSIONS

To clarify the effect of earthquake-induced settlement of clay layer on the ground subsidence, the settlement-time relations for the separate layers in the ground were observed and by the multi-directional simple shear tests the direction of cyclic shear on the settlement of clay was investigated. In conclusion, following results were obtained.

- 1) For the settlement of the alluvial clay layer in the Port Island induced by the Hyogo-ken Nanbu Earthquake, the settlement over 4cm was predicted.
- 2) The effects of the direction of cyclic shear on the post-earthquake settlement are not negligible.
- 3) The larger the phase difference in the sinusoidal shear strains from two directions, the smaller the effective stress.
- 4) When a clay is subjected to the multi-directional shear strain, the settlement in the reconsolidation stage is also affected by the phase difference.

ACKNOWLEDGEMENT

The settlement-time relations at Port Island reported in this study were offered by the Kobe Municipal Office and the accelerograms at the Port Island were supplied by the Committee of Earthquake Observation and Research in the Kansai Area. The authors would like to express their gratitude for their help to this study.

REFERENCES

- Jaime, A. P, Romo, M. P. and Jasso, M. R. (1987), "Seismic Induced Settlement in a Building", *8th Pan-American Congress on Soil Mechanics and Foundation Engineering* , pp 257-275.
- Lee, K. L. and Albaisa, A. (1974), "Earthquake induced settlements in saturated sands", *Journal of the Geotechnical Engineering Division, ASCE*, 100, GT4, pp387-406.
- Matsui, T. (1995), "*The seabed ground, Kaiteijiban*", *Japanese Geotechnical Society, Kansai Branch*. (in Japanese)
- Matsuda, H. and O-hara, S. (1990), "Geotechnical Aspects of Earthquake-Induced Settlement of Clay Layer", *Marine Geotechnology*, 9, pp179-206.
- Matsuda, H. and Shimizu, Y. (1996), "Seismic ground subsidence in near-shore reclaimed land", *The Kobe Earthquake Geodynamical Aspects, Computational Mechanics Publications, Southampton, UK*, pp73-98.
- Matsuda, H. (1997), "Estimation of Post-Earthquake Settlement-Time Relations of Clay Layers", *Journal of Geotechnical Engineering*, 568/III, pp41-48. (in Japanese)
- Matsuda, H. and Nagira, H. (1998), "Estimation of the post-earthquake subsidence in clay layers", *6th U.S. National Conference on Earthquake Engineering*, 134, pp1-11.
- Matsuda, H. and Emoto, N. (1998), "Effect of direction of earthquake motion on settlement of clay layer", *The 10th Earthquake Engineering Symposium, Proceedings*, 2, pp1427-1432. (in Japanese)
- Nagase, H. & Ishihara, K. (1988), "Liquefaction-induced compaction and settlement of sand during earthquakes", *Journal of the Japanese Society of Soil Mechanics and Foundation Engineering, Soils and Foundations*, 28 1, pp65-76.
- O-hara, S. and Matsuda, H. (1988), "Study on the Settlement of Saturated Clay Layer Induced by Cyclic Shear", *Soils and Foundations* 28, 3, pp103-113.
- Pyke, R., Seed, H. B. and Chan, C. K. (1975) , "Settlement of sands under multidirectional shaking", *Journal of the Geotechnical Engineering Division, ASCE*, 101, GT4, pp379-398.
- Seed, H. B. and Silver, M. L. (1972), "Settlement of dry sands during earthquakes", *Journal of the Geotechnical Engineering Division, ASCE*, 98, SM4, pp381-397.
- Suzuki, T. (1984), "Settlement of Saturated Clays under Dynamic Stress History", *Journal of the Japan Society of Engineering Geology* 25, 3, pp21-31. (in Japanese)
- Tanimoto, K. and Tamura, K. (1989), "Settlement characteristics of coastal reclaimed land", *The construction Engineering Research Institute Foundation*, 31, pp229-243. (in Japanese)
- The Committee of Earthquake Observation and Research in the Kansai Area (GEORKA), (1995), *The Distributed Seismic Records and Data*. (in Japanese)
- Zeevaert, L. (1972), *Foundation Engineering for Difficult Subsoil Conditions, New York, Van Nostrand Reinhold Company*.